Int. J. Heat Mass Transfer. Vol. 17, pp. 1329–1336. Pergamon Press 1974. Printed in Great Britain

NUMERICAL PREDICTIONS FOR TURBULENT FREE CONVECTION FROM VERTICAL SURFACES

H. B. MASON* and R. A. SEBAN†

(*Received* 7 *November* 1973)

Abstract—Numerical calculations for the free convection heat transfer from vertical surfaces have been made by means of suitable modifications of a program of the Patankar–Spalding type, and the heat-transfer coefficients so predicted, by the use of turbulence parameters successful for the prediction of forced convection flows, are shown to agree fairly with available results for air, water, and oils for both isothermal walls and those producing a constant rate of heat transfer.

NOMENCLATURE

a, constant in relation for turbulent viscosity, equation (8);
b, constant in relation for turbulent energy dissipation, equation (9);
e, turbulent kinetic energy $\frac{1}{2}(\overline{u'^2}+\overline{v'^2}+\overline{w'^2})$;
g, gravity acceleration;
h, heat-transfer coefficient;
i, enthalpy;
k, thermal conductivity;
l, mixing length;
p, pressure;
q, heat flux at wall;
r, radius, axisymmetric system;
T, temperature;
u, v, mean velocity components in x and y directions;
u_m, maximum velocity in the boundary layer at any location;
u', v', w', turbulent velocity components;
x, distance from leading edge along surface;
y, distance normal to surface.

Greek symbols

α, thermal diffusivity;
δ, boundary-layer thickness;
κ, Karman constant;
λ, ratio of outer mixing length to boundary-layer thickness;
μ, viscosity;
μ_t, turbulent viscosity;
ν, kinematic viscosity;
ρ, density;
σ, Prandtl number;
σ_t, turbulent Prandtl number for thermal energy;
σ_e, turbulent Prandtl number for kinetic energy of turbulence;
τ, shear stress;
ψ, stream function.

Subscripts

w, wall, $y = 0$;
∞, in the ambient fluid.

INTRODUCTION

TURBULENT free convection from a vertical plate has been measured by many experimentors and recent results have included velocity and temperature profiles in the boundary layer. Cheesewright [1] and Warner [2] have given results for air, on an isothermal plate, Vliet and Liu [3] for water and constant heat rate, and Fujii [4] for water and oils on a vertical cylinder (the curvature affect was not significant) for both isothermal and constant heat rate conditions. Fujii found that the relationship of the local Nusselt number to the local Rayleigh number was the same for these two boundary conditions.

Eckert and Jackson [5] were the first to make predictions of turbulent free convection by means of the integral method, via assumptions about the velocity and temperature profiles and friction and heat-transfer laws. Recently, Kato [6] applied the integral method by assuming an eddy diffusivity relationship and a distribution of the heat flux across the boundary layer and so derived the profiles of velocity and temperature instead of assuming them. The results for the local Nusselt number are not very different from those of Eckert and Jackson, though Fujii shows that his

*Present address: Aerotherm Acurex Corporation, Mountain View, California, U.S.A.
†Professor of Mechanical Engineering, University of California at Berkeley, Berkeley, California, U.S.A.

results conform better to the predictions of Kato. The velocity profiles predicted by Kato are only slightly different than the Eckert and Jackson profile but the temperature distributions show a substantial change and Kato showed that his predictions conformed better to earlier measurements that were made by Fujii.

The availability of convenient methods for numerical solution of the boundary-layer equations removes the need for the kinds of assumptions associated with integral methods and provides the potential for the solution of a wide variety of problems, as has been widely demonstrated in respect to forced convection systems. This paper shows the results that can be obtained from a program of the type developed by Patankar and Spalding [7] in the prediction of the results of the experimentors to which reference has been made.

EQUATIONS

The continuity, momentum and energy equations are taken in their usual forms for a single component turbulent boundary-layer flow, with the turbulent stress given as $\mu_t(\partial u/\partial y)$ and the turbulent heat flux as $(\mu_t/\sigma_t)c(\partial T/\partial y)$.

$$\frac{\partial(\rho u r)}{\partial x}+\frac{\partial(\rho v r)}{\partial y}=0 \tag{1}$$

$$\rho u\frac{\partial u}{\partial x}+\rho v\frac{\partial u}{\partial y}=\frac{1}{r}\frac{\partial}{\partial y}\left[r(\mu+\mu_t)\frac{\partial u}{\partial y}\right]-\frac{\mathrm{d}p}{\mathrm{d}x}-\rho g \tag{2}$$

$$\rho u\frac{\partial i}{\partial x}+\rho v\frac{\partial i}{\partial y}=\frac{1}{r}\frac{\partial}{\partial y}\left[r\left(\frac{\mu}{\sigma}+\frac{\mu_t}{\sigma_t}\right)\frac{\partial i}{\partial y}\right]. \tag{3}$$

Here x is the upward directed distance, y the distance normal to the surface and r the radius of the axisymmetric system that is assumed. The equations for the two dimensional case are those above with r taken to be unity. The pressure, uniform in y by the boundary-layer assumptions, is given by $\mathrm{d}p/\mathrm{d}x=-\rho_\infty g$. Dissipation has been neglected and "i" is used for the enthalpy to avoid confusion with the local heat-transfer coefficient, h.

NUMERICAL SOLUTION

The essence of the Genmix [7] program is the transformation of the above equations to the independent variables (x,ω) with $\omega=(\psi-\psi_I)/(\psi_E-\psi_I)$, where ψ is the stream function and subscripts I and E specify its value at the surface (here impermeable so that $\psi_I=0$), and at the outer edge of the layer. Reference [7] gives the details of the numerical approximation and [8] contains some of them also, together with additional considerations relative to the free convection problem and the listing that was used to obtain the results that are presented here.

For laminar flows ($\mu_t=0$), the only prescriptions needed are the grid distribution and the entrainment. Stability is aided by an ω distribution with increments $\Delta\omega$ increasing monotonically from the wall outward, though this produces very large increments Δy near the outer edge of the layer where the velocity approaches the zero value of the ambient region. The external entrainment is specified by the assumption of a parabolic velocity distribution at the outer edge of the layer. This, substituted into an approximate form of equation (2) for this region, gives ultimately the form

$$(\rho v r)_E=\frac{-2[r(\mu+\mu_t)]_N+[r\mu]_{NP3}}{y_{NP3}-y_N}. \tag{4}$$

Here N denotes the second grid point measured inward from the external boundary which is at $NP3$. The use of equation (4) gives results not much different from alternatives thereto, one of which is to so arrange the calculation for the outermost increment that the velocity at the fictive outer point ($NP2$) remains essentially zero. It is to be noted that the entrainment specification, of only incidental concern when the outer velocity is finite, has a critical influence on the solution when the outer velocity is zero, as occurs in the problem of jets and of free convection in an ambient environment.

The application to laminar convection from a vertical isothermal plate used 41 points across the layer and the necessary initial conditions from the Ostrach [9] solution at a small value of x. The calculation, carried out to much larger values of x, reproduced that solution for the surface characteristics (shear and heat-transfer coefficient) very closely. Similar results were obtained for the plate with constant flux, for a thin isothermal cylinder [10], and an isothermal cone of 60° apex angle [11] for which the body force term in equation (2) was suitably altered. Some deviation is apparent near the outer edge of the layer, where the numerical solution gives velocity and temperature profiles decaying to the free stream values slightly more rapidly than the asymptotic approach of the analytical solution. In total, these results for laminar flow were taken to confirm the essential validity of the method.

TURBULENT FLOW

Contrasted to the laminar flow situation, the use of the program for turbulent flow requires additions and the specification of many parameters, the selection of the latter being guided by those values which already have been successfully used in forced flow situations.

The entrainment specification was retained, as equation (4).

The turbulent viscosity can be specified by the "Prandtl mixing length" hypothesis, with the mixing

length specified according to van Dreist for the region near the wall

$$\mu_t = \rho l^2 \frac{\partial u}{\partial y} \tag{5}$$

$$l = \kappa y\left[1-\exp\left(-\frac{\sqrt{(\tau_w\rho)}\cdot y}{26\mu}\right)\right] \tag{6}$$

and away from the wall, $\kappa y > \lambda y_{NP3}$

$$l = \lambda y_{NP3} \qquad \lambda = 0{\cdot}09. \tag{7}$$

The turbulent Prandtl number for energy transfer was taken to be

$$\sigma_t = 0{\cdot}85 \quad \text{for} \quad \kappa y < \lambda y_{NP3}$$
$$\sigma_t = 0{\cdot}50 \qquad \kappa y > \lambda y_{NP3}.$$

The use of the Prandtl mixing length reduces μ_t to zero at the velocity maximum and to small values in this locality and one means for avoiding this contradiction is the specification of the turbulent viscosity in terms of the turbulent kinetic energy as:

$$\mu_t = a\rho l e^{1/2} \qquad e = \tfrac{1}{2}(\overline{u'^2}+\overline{v'^2}+\overline{w'^2}). \tag{8}$$

Here "a" is a constant to be selected and "l" the mixing length, for which the specifications of equations (5) and (7) are retained. The turbulent kinetic energy is determined from a conservation equation that is somewhat arbitrarily arrived at (8)

$$\rho u\frac{\partial e}{\partial x}+\rho v\frac{\partial e}{\partial y} = \frac{1}{r}\frac{\partial}{\partial y}\left[r\left(\mu+\frac{\mu_t}{\sigma_e}\right)\frac{\partial e}{\partial y}\right] + \mu_t\left(\frac{\partial u}{\partial y}\right)^2 - \frac{b\rho e^{3/2}}{l} - \overline{\rho' u'}g. \tag{9}$$

Forcing this form introduces the additional parameter of a turbulent Prandtl number for kinetic energy transfer, σ_e, and introduces the semi-empirical expression, $be^{3/2}/l$, for the dissipation of turbulent kinetic energy, with its constant, b. The final term, $\overline{\rho' u'}g$, was usually ignored; an overestimate, whereby $\overline{\rho' u'}$ was taken to be $\overline{\rho' v'}$, so that

$$\overline{\rho' u'}g = -g\frac{\mu_t}{\sigma_t}\frac{\mathrm{d}T}{\mathrm{d}y},$$

was attempted for air and for water. It produced a slight increase in the turbulence level but a negligible effect upon the heat-transfer coefficient.

For the Prandtl mixing length (PML) calculation, the preservation of computational stability required the retention of an ω spacing like that used for laminar flow, with $\Delta\omega$ increasing with y. With the turbulent kinetic energy (TKE) calculation, however, it was found that a spacing:

$$\omega = \sin^3\left[\frac{\pi}{2}\left(\frac{I-2}{NP2-2}\right)\right] \tag{10}$$

did produce stable solutions and the small $\Delta\omega$ near the outer edge of the layer that is achieved in this way provided the reasonably small increments in y near the outer edge of the layer which could not be obtained with the PML calculation.

The grid distributions that were used were dense enough in the wall region so that the point nearest the wall, at $I = 3$, always involved a value of $(y/\mu)\sqrt{(\tau_w\rho)}$ that was unity or less, so that the transport in this region could be assumed to be molecular and the wall function for this region could be taken as for laminar flow.

The initial conditions were taken well below the point of transition, and were those of a suitable analytic solution for laminar flow. The transition point was assumed at a value implied by the data to which comparisons were made and at this point the initial turbulent kinetic energy distribution was obtained by taking to be zero all terms in equation (9) except the second and third on the right (equal production and dissipation of the turbulent energy). This artificially initiated the turbulent kinetic energy calculation according to equation (8) without excessive oscillation but this artifice of course ignores the complicated transition process that has been so well described by Fujii [4].

All the calculations involved variable properties, with those for air employing standard values and those for water and oil the algebraic specifications of Fujii [4]. All results are expressed in terms of properties evaluated at a reference temperature $T_r = 0{\cdot}5(T_w + T_\infty)$. Then the calculations could be made for the operating conditions of the experiment once κ, λ, and σ_t were chosen for a PML calculation and when in addition a, b, and σ_e were chosen if, as in almost all cases, the TKE method was employed. A substantial exploration of values in which the results were compared to experimental values for air indicated that the values $a = 0{\cdot}5$, $b = 0{\cdot}125$, $\sigma_e = 1{\cdot}7$ for $\kappa y < \lambda y_{NP3}$ and $\sigma_e = 0{\cdot}7$ for $\kappa y > \lambda y_{NP3}$ gave acceptable results. The sensitivity to these values is not too great, and the values $a = 0{\cdot}55$, $b = 0{\cdot}164$, $\sigma_e = 1$ gave almost the same results for the local heat-transfer coefficient.

RESULTS

Figure 1 shows some of the results given by computations made for the conditions shown on Table 1, to correspond to the operating conditions for various experiments. All properties are taken at a reference temperature which is the average of wall and free stream temperatures and the heat-transfer coefficient is shown in terms of the ratio of the Nusselt number to the cube root of the Prandtl number in order to obtain a compact representation for these results. The results

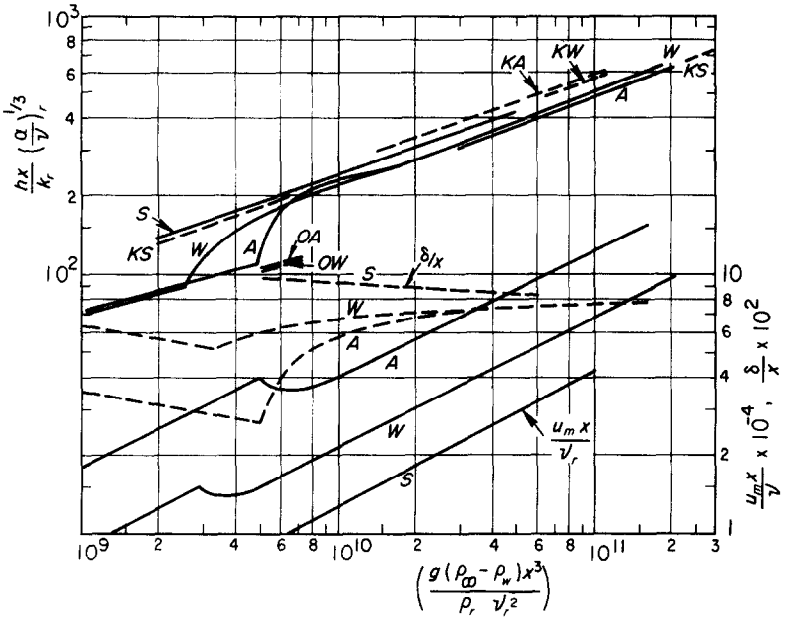

FIG. 1. Predictions for turbulent free convection, isothermal wall. Curve A—Run A-10, Table 1, air $Pr_r = 0{\cdot}73$; Curve W—Run W-1, Table 1, water $Pr_r = 5{\cdot}81$; Curve S—Run S-1, Table 1, spindle oil $Pr_r = 58{\cdot}7$; Curves OA, OW, Ostrach laminar, air and water; Curves KA, KW, KS Kato turbulent, air, water, spindle oil.

Table 1

Run	T_w (°K)	T_∞ (°K)	q_w (W/m²)	$(Gr)_r$ trans.		Pr_r	Experiment	Fluid
A-10	335	298		5×10^9	TKE	0·73	Warner	air
A-2	335	298		5×10^9	PML	0·73	Warner	air
W-1	308	293		$2{\cdot}6 \times 10^9$	TKE	5·87	Fujii	water
W-2		295	6810	1×10^{10}	TKE	$\simeq$ 5·6	Vliet	water
S-1a	370	309		5×10^8	TKE	58·7	Fujii	spindle oil
S-2		313	9500	7×10^8	TKE	$\simeq$ 56	Fujii	spindle oil
M-1	424	333		$1{\cdot}2 \times 10^9$	TKE	75	Fujii	Mobiltherm

for air and water are close on this basis, and the result for oil is higher.

These results for the heat-transfer coefficient can be compared to the isothermal results of Kato by means of his empirical specification of his analytical results:

$$\frac{hx}{k} = 0{\cdot}149\left(\left(\frac{\nu}{\alpha}\right)^{0{\cdot}175} - 0{\cdot}55\right)\left(\frac{g(\rho_\infty - \rho_w)x^3}{\rho\nu^2}\right)^{0{\cdot}36}. \quad (11)$$

As shown on Fig. 1 the indication from equation (11) for the Prandtl numbers involved on that figure is about 20 per cent above the prediction for air and water and about 12 per cent below the prediction for the oil. This comparison, however, implies that the chosen reference temperature is appropriate and it is noted in the following discussion on Fig. 3 that for the oil the preferred reference temperature according to Fujii would reduce the ordinate of the prediction to achieve correspondence with the Kato prediction. The differences that exist on Fig. 1 for air and water would, however, remain.

In the presently predicted results, and in the experimental ones which follow, the distance x is always taken as that from the origin of the initially laminar flow, in the view that the transition behavior itself, combined with the distance downstream from transition, results in the layer behaving as though it had been turbulent from $x = 0$ onwards. Ideally comparisons should not be made on this basis, but rather with a boundary-layer thickness dimension supplanting the length dimension, but it is impossible to treat the available data on this basis.

Figure 1 also shows the laminar predictions of Ostrach for air and for water ($Pr = 5{\cdot}8$) and indicates the predictions to be close to them. The prediction for the oil ($Pr = 58$) is not shown but this variable property prediction is in similar agreement if Fujii's reference temperature is used with it.

Figure 1 shows also the maximum velocity in the boundary layer in the group $u_m x/\nu_r$, which follows a power law variation such that u_m is approximately proportional to $x^{0{\cdot}55}$. The boundary-layer thickness $\delta = y_{NP3}$, is shown as δ/x and this does not follow a power law within the region of the results, though this ratio appears to become asymptotic to a value of about 8×10^{-2}, so that perhaps ultimately $\delta \sim x$. These dependencies can be contrasted to those found by Eckert and Jackson [5]: $h \sim x^{1/5}$, $u_m \sim x^{1/2}$, $\delta \sim x^{7/10}$, but no comparison really is possible because the present results did not give similar velocity and temperature profiles up to the maximum values of Grashof number for which the predictions were made, though those for air nearly become so.

Figure 2 shows values of the ratio of turbulent to laminar viscosity μ_t/μ at the position where $u/u_m = 0{\cdot}50$ on the outside of the velocity maximum. Here this viscosity ratio is almost at its maximum. The ratio is also shown at the position of the velocity maximum and at a position this close to the wall the ratio is very much lower; for air at the highest Grashof number it attains only a value of 4. For spindle oil the values of the ratio are relatively low but it must be recalled that its influence on the temperature distribution is in proportion to $(\mu_t/\mu)(\nu/\alpha)$.

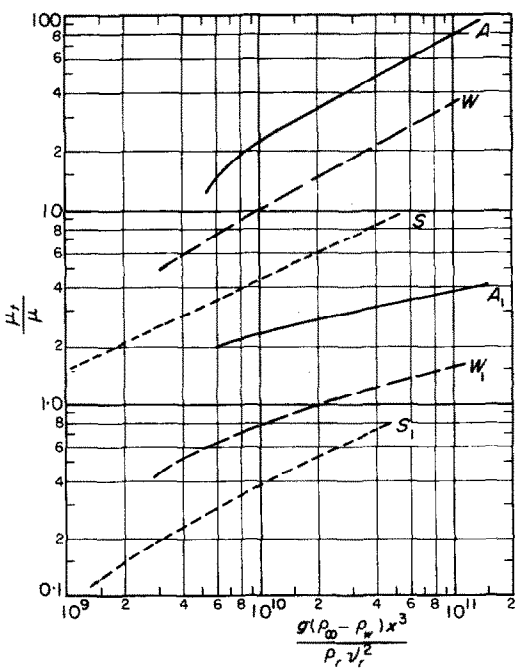

FIG. 2. Ratio of turbulent to laminar viscosity. Upper curves, where $u/u_m = 0{\cdot}50$, outer part of layer; lower curves, at velocity maximum. Runs of Fig. 1.

NUSSELT NUMBER

Figure 3 shows curves by which the various experimentors have correlated their results, adjusted as necessary for a reference temperature which is the mean of the wall and free stream values, which in turn are typical of those used in the experiments. The length of these lines on Fig. 3 corresponds approximately to the experimental range.

Curves WA and PA indicate the results of Warner [2] and of Pirovano [12] for air. Cheesewright's results cover the same range but are about 20 per cent higher. Curve A is the prediction, closest to the Warner result.

Curve VW is the Vliet result for water, $Nu_r = 0{\cdot}058\,(Gr\,.\,Nu\,.\,Pr)_r^{0{\cdot}22}$, evaluated for $Pr = 5{\cdot}8$, and curve FW is Fujii result for water $(Nu)_r = 0{\cdot}13\,(GrPr)_r^{1/3}$ (the same for an isothermal wall and for constant heat rate) evaluated for $Pr = 5{\cdot}8$, and shifted to compensate for the difference in reference temperature. Fujii indicated that $t_r = 0{\cdot}75t_w + 0{\cdot}25t_\infty$(°C) was preferable to $t_r = (t_w + t_\infty)/2$ and for the condition of run W-1 of Table 1 this increases the factor 0·13 by the factor 1·03.

The numerical results for the Nusselt number for run W-2, for constant heat rate, are essentially the same as for W-1 at the same Grashof number, confirming Fujii's experimental conclusion. Thus the curve W of Fig. 3 represents both runs W-1 and W-2. It is about 20 per cent below the Fujii result and is about equally above and below the Vliet result because of the radically lower Grashof number exponent of the Vliet correlation.

For spindle oil Fujii gave $Nu = 0{\cdot}015\,(GrPr)^{0{\cdot}4}$ for the highest Grashof numbers (both for isothermal and constant heat rate) and the adjustment for the reference temperature introduces an additional factor of 1·12 into the representation, line FS, of this relation for the condition of run S-1. (The visibility of this line is low because it crosses and almost coincides with line W.) The prediction, S, is about 10 per cent high.

Figure 3 also contains another appraisal for air, for which curve A is repeated to contrast with curves 1 and 2. Curve 1 refers to a prediction with stratified ambient conditions, corresponding to $(297 + 2{\cdot}11x)$°K and shows as a consequence an increase in the heat-transfer coefficient. Since Warner had this kind of stratification this comparison implies that his results may be slightly high because of it.

Curve 2 of Fig. 3 shows the result obtained from run A-2, comparable to A-10 except for the use of the Prandtl mixing length to obtain the turbulent viscosity.

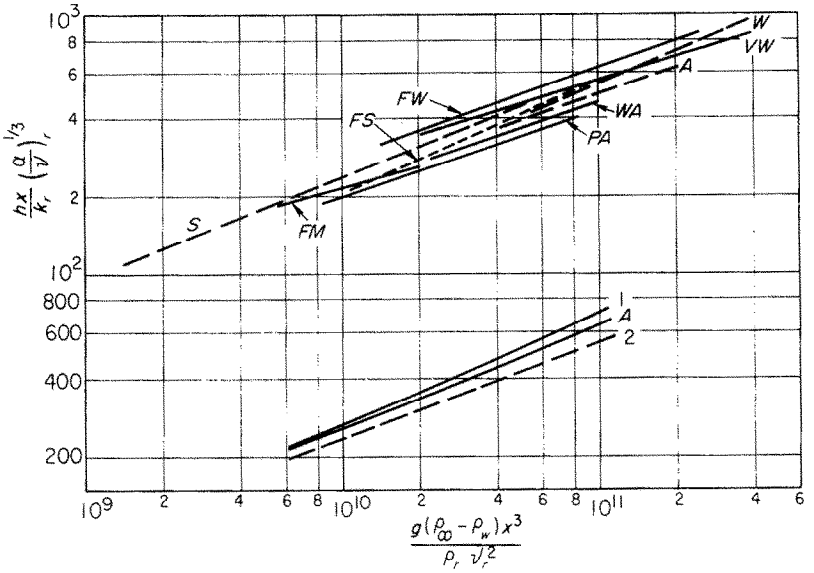

FIG. 3. The local Nusselt numbers from various experiments. Air: *PA*, Pirovano; *WA*, Warner, $Pr_r = 0{\cdot}73$; water: *VW*, Vliet; *FW*, Fujii, $Pr_r = 5{\cdot}8$; spindle oil: *FS*, Fujii, $Pr_r = 58$; Mobiltherm oil: *FM*, Fujii, $Pr_r = 75$; curve: *A*, Run *A*-10; *W*, Run *W*-1 or *W*-2; *S*, Run *S*-1 or *S*-2; 1, Run *A* with stratification; 2, *A* with Prandtl mixing length.

The lower heat-transfer coefficients so obtained are due to the fact that μ_t then vanishes at the velocity maximum, the undesirable feature that indicated the use of the TKE method in all of the other calculations.

VELOCITY PROFILES

Figure 4 is the presentation made by Cheesewright for three of his velocity profiles, with coordinates chosen on the basis of the power law relationships given by the Eckert and Jackson analysis. The predictions, for similar operating conditions and for $x = 2{\cdot}6$ m, show larger values of the velocity maximum but are otherwise in general accord with the forms of the data. Not too much can be made of this comparison in view of the fact that, as already noted, the predicted heat-transfer coefficients are considerably below the values that were obtained by Cheesewright.

Figure 5 shows two of the velocity profiles obtained by Vliet [3] with water and demonstrates that the correspondence with prediction is much better than that indicated by Fig. 4 for air, though for the uppermost profile there is a considerable discrepancy near the outer edge of the layer. As a matter of interest, there are shown also Vliet's measurements for the x component of turbulent kinetic energy, shown as $\sqrt{(\overline{u'u'})}/u_m$, and the total kinetic energy of the prediction, given as

$$\frac{1}{u_m}\left[\tfrac{1}{2}(\overline{u'^2}+\overline{v'^2}+\overline{w'^2})\right]^{1/2}.$$

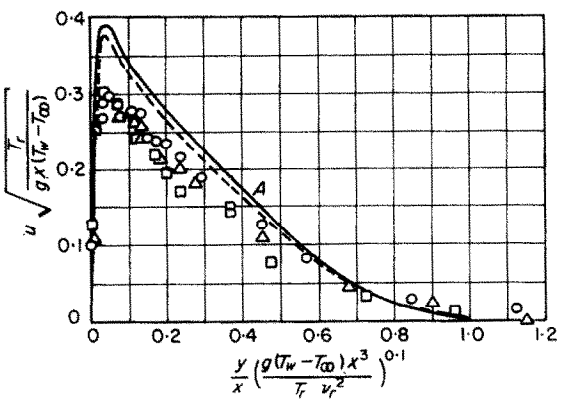

FIG. 4. Velocity profiles by Cheesewright for air.

Points	x	T_w	T_∞
	2·0	334	299°K
	2·01	330	300°K
	2·6	356	300°K

Curves: *A*, isothermal ambient at $x = 2{\cdot}14$ m; *B* same, stratified ambient corresponding to experimental conditions.

With isotropic turbulence, the latter should be 20 per cent greater than the former. At $x = 0{\cdot}76$ m it is less, and at $x = 1{\cdot}07$ m it is greater. Even a magnitude correspondence is encouraging, and the portrayal of the prediction on Fig. 5 also demonstrates the distribution of turbulent kinetic energy typical of all of the predictions.

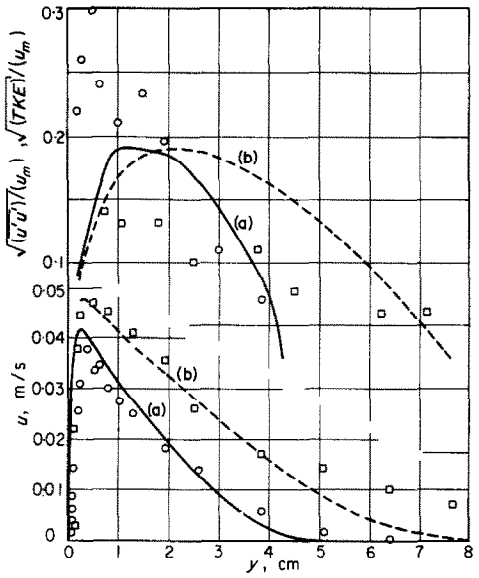

FIG. 5. Velocity and turbulent energy profiles by Vliet for water.

Points experiment	x (m)	q_w (W/m^2)	T_∞ (°K)	Curves theory
circle	0·76	6810	295	(a)
square	1·07	6810	295	(b)

TEMPERATURE PROFILES

While the velocity profiles are not greatly different than the assumption of Eckert and Jackson,

$$\frac{u}{u_m} = 1{\cdot}86\left(\frac{y}{\delta}\right)^{1/7}\left(1-\frac{y}{\delta}\right)^4,$$

Fujii has noted the substantial difference between the experimental temperature profile and the assumed profile of $(T-T_\infty)/(T_w-T_\infty) = 1-(y/\delta)^{1/7}$. Fujii gave algebraic forms to fit his results for water and oil and proposed one to fit the temperature distribution measured by Cheesewright in air. These are shown as curves on Fig. 6 and in view of the average that must be taken of the very large temperature fluctuations that are demonstrated by Fujii, these curves are probably as satisfactory a representation as are the data points themselves. The figure contains also, as points, the temperature distributions predicted for high Grashof numbers for the runs made for air, water and oil, and these points are marked by an arrow to indicate the position of the velocity maximum. The correspondence is good. Reference [8] shows that the prediction for air corresponds with Warner's measurements of the temperature profile to a slightly better degree than does the comparison for air that is shown on Fig. 6.

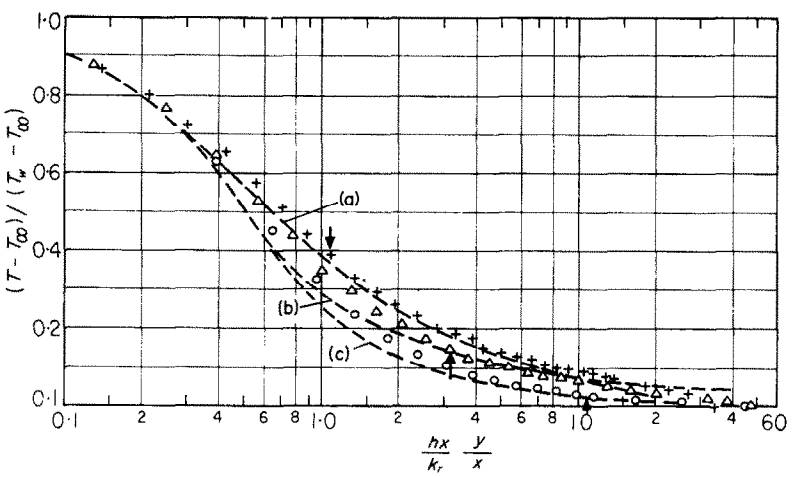

FIG. 6. Temperature profiles, isothermal wall.

Curves (Fujii)	points (prediction)	run	Grashof
(a) air	plus	A-10	$1{\cdot}16 \times 10^{11}$
(b) water	triangle	W-1	$1{\cdot}87 \times 10^{11}$
(c) spindle oil	circle	S-1	$3{\cdot}4 \times 10^{10}$

The arrows show the location of the velocity maximum.

CONCLUSIONS

Predictions of free convection heat-transfer coefficients, and of temperature and velocity profiles, made from a numerical solution of the boundary-layer equations, have been shown to compare with available experimental results to a degree better than most theories and about as well as the integral method of Kato [6]. This supports the further use of the numerical method for many free convective problems in turbulent flow and it is noteworthy that this has been partially done in [8], where favorable comparisons are also shown for combined natural and rotational convection from a rotating cone and for plumes in uniform and stratified surroundings.

Acknowledgement—The computations were made possible by time provided by the Computer Center of the University of California at Berkeley.

REFERENCES

1. R. Cheesewright, Natural convection from a vertical plane surface, *J. Heat Transfer* **90**, 1 (1968).
2. C. Y. Warner, Turbulent natural convection in air along a vertical flat plate, *Int. J. Heat Mass Transfer* **11**(3), 397 (1968).
3. G. C. Vliet and C. K. Liu, An experimental study of turbulent natural convection boundary layers, *J. Heat Transfer* **91**, 511 (1969).
4. T. Fujii, M. Takeuchi, M. Fujii, K. Suzaki and H. Vehara, Experiments on natural convection heat transfer from the outer surface of a vertical cylinder to liquids, *Int. J. Heat Mass Transfer* **13**, 753 (1970).
5. E. R. G. Eckert and T. W. Jackson, Analysis of turbulent free-convection boundary layer on a flat plate, NACA TR 1015 (1951).
6. H. Kato, N. Nishiwaki and M. Hirata, On the turbulent heat transfer by free convection from a vertical plate, *Int. J. Heat Mass Transfer* **11**, 1117–1125 (1968).
7. S. V. Patankar and D. B. Spalding, *Heat and Mass Transfer in Boundary Layers*, 2nd Edn. Intertext Books, London (1970).
8. H. B. Mason, Numerical computation of steady natural convective flows with rotation and stratification, Ph.D. Thesis, University of California, Berkeley, California (1971).
9. S. Ostrach, An analysis of laminar free-convection flow and heat transfer about a flat plate parallel to the direction of the generating body force, NACA TR 1111 (1953).
10. E. M. Sparrow and J. L. Gregg, Laminar free convection heat transfer from the outer surface of a vertical circular cylinder, *Trans. Am. Soc. Mech. Engrs* **78**, 1823 (1956).
11. R. G. Hering and R. J. Grosh, Laminar free convection from a non-isothermal cone, *Int. J. Heat Mass Transfer* **5**, 1059 (1962).
12. A. Pirovano, S. Viannay and M. Jannot, Convection naturelle en regime turbulent le long d'une plaque plane verticale, in *Heat Transfer 1970*, Vol. 4, Paper NC 1.8. Elsevier, Amsterdam (1970).

ESTIMATION NUMERIQUE DE LA CONVECTION NATURELLE TURBULENTE LE LONG DES SURFACES VERTICALES

Résumé—Des calculs numériques de la convection thermique naturelle par des surfaces verticales sont faits à partir de modifications convenables d'un programme du type Patankar–Spalding. Les coefficients de convection, calculés en utilisant les paramètres de turbulence introduits avec succès en convection forcée, s'accordent avec les résultats connus sur l'air, l'eau, les huiles aussi bien pour des parois isothermes que pour un flux pariétal constant.

NUMERISCHE BERECHNUNGEN TURBULENTER FREIER KONVEKTION AN SENKRECHTEN OBERFLÄCHEN

Zusammenfassung—Es wurden numerische Berechnungen des Wärmeübergangs bei freier Konvektion an senkrechten Oberflächen mittels geeigneter Modifikationen eines Programms nach Patankar–Spalding durchgeführt. Es wird gezeigt, daß die so bestimmten Wärmeübergangskoeffizienten für Luft, Wasser und Öle gut mit bekannten Versuchsergebnissen übereinstimmen, wenn man Turbulenz-Parameter benutzt, die erfolgreich zur Berechnung von Strömungen mit erzwungener Konvektion verwendet wurden. Diese Übereinstimmung ist sowohl für isotherme als auch für Wände mit konstantem Wärmestrom gegeben.

ЧИСЛЕННЫЕ РАСЧЕТЫ ТУРБУЛЕНТНОЙ СВОБОДНОЙ КОНВЕКЦИИ ОТ ВЕРТИКАЛЬНЫХ ПОВЕРХНОСТЕЙ

Аннотация — С помощью соответствующих модификаций программ типа Патанкара–Сполдинга проведены численные расчеты теплообмена при свободной конвекции от вертикальных поверхностей. Показано, что рассчитанные таким образом коэффициенты тепло обмена с использованием параметров турбулентности для вынужденной конвекции хорошо согласуются с имеющимися данными для воздуха, воды и масел как для изотермических стенок, так и тех, которые обеспечивают постоянную скорость теплообмена.